SOME CHEMICAL AND MINERALOGICAL CHARACTERISTICS OF TONSTEINS AND BENTONITES IN NORTHEAST BRITISH COLUMBIA (93O, P, I; 94A)

By W. E. Kilby

INTRODUCTION

Tonsteins and bentonites were first reported from the Peace River Coalfield by Duff and Gilchrist (1983) who demonstrated that these altered volcanic ash bands were laterally continuous. Tonsteins have been used successfully for stratigraphic correlation in several regions of the world, most notably the Westphalian coal measures of western Europe and Britain, because they are deposited so rapidly that they are essentially 'time lines.' It was for the purpose of regional and local correlation that the current tonstein and bentonite study was initiated by the Ministry in 1983. To date some 460 samples have been collected of which 416 have been analysed by X-ray diffraction and 101 chemically. These samples were collected from coal-bearing and contiguous formations of the coalfield. Previous articles have discussed outcrop and thin-section characteristics (Kilby, 1984a) and local to regional correlations based on stratigraphic position and geophysical log signature (Kilby, 1985).

This paper focuses on the chemical and mineralogical characteristics of these ash bands. A method of digitally representing and utilizing X-ray diffractogram data for mineral and chemical quantification has been developed and is presented here. It is essential to gain a firm understanding of these characteristics if any meaningful correlation techniques based on mineral or chemical parameters are to be developed. Tonsteins and bentonites are mineralogically different but have, in some instances, originated from the same ash fall (Kilby, 1984a). Tonsteins are kaolinite rich and occur in or near coal seams, whereas bentonites are smectite rich and associated with marine strata. Late diagenic or tectonic carbonatization has complicated the chemical and mineralogical characteristics of some samples.

Studies this past field season focused on extending the area over which the Fisher Creek tonstein zone could be correlated. Legun (pers. comm.) discovered a surface showing of this zone along Gaylard Creek about 10 kilometres west of the W.A.C. Bennett Dam; the zone was about 20 metres below the Moosebar Formation at this location. A similar tonstein zone was found along the south side of the Murray River about 4 kilometres west of the Quintette plant site. Identification of the stratigraphic interval thought to contain the tonstein zone in this area was made on geophysical logs from rotary borehole QBR-8118 which led to its location in surface exposure. Core searches yielded several occurrences of tonsteins at the suspected stratigraphic horizon from holes on the Monkman property. Proving that these are the Fisher Creek tonstein zone would establish a lateral correlation of approximately 160 kilometres. Isochronous marker horizons on this scale provide an excellent framework on which to base coal rank, stratigraphic, and microfossil studies.

CHEMISTRY

Forty-three new tonstein and bentonite chemical analyses were received during 1985, and P_2O_5 values for 17 of the samples reported in Kilby (1985). Table 20-1 contains the results for all 43 new samples and the other 17 samples for which new information became available. Figure 20-1 shows the correlation matrix of 13

SiO_2	Al_2O_3	Fe_2O_3	MgO	CAO	Na_2O	K_2O	TiO_2	MnO	P_2O_5	Rb	Sr	Zr	
0	.387	-.625	-.797	-.797	.223	.195	.319	-.32	-.416	.065	-.223	-.127	SiO_2
0	0	-.478	-.735	-.69	-.378	-.297	.29	-.216	-.041	-.165	-.262	.132	
0	0	0	.358	.3	-.067	-.038	-.283	.426	.162	.031	.046	.158	•
0	0	0	0	.974	.083	-.03	-.3	.206	.26	-.016	.311	-.081	
0	0	0	0	0	-.003	-.086	-.278	.161	.358	-.062	.346	-.076	
0	0	0	0	0	0	.362	-.19	.075	-.341	.242	.014	-.029	
0	0	0	0	0	0	0	-.399	0	-.342	.745	-.022	.047	•
0	0	0	0	0	0	0	0	-.103	-.049	-.515	-.029	-.113	
0	0	0	0	0	0	0	0	0	-.015	.087	0	.01	
0	0	0	0	0	0	0	0	0	0	-.247	.415	.126	•
0	0	0	0	0	0	0	0	0	0	0	.055	.273	
0	0	0	0	0	0	0	0	0	0	0	0	-.087	
0	0	0	0	0	0	0	0	0	0	0	0	0	Zr

Figure 20-1. Chemical correlation matrix for 13 elements determined for 101 samples.

British Columbia Ministry of Energy, Mines and Petroleum Resources, Geological Fieldwork, 1985, Paper 1986-1.

TABLE 20-1. CHEMICAL ANALYSES OF TONSTEINS AND BENTONITES, PEACE RIVER COALFIELD

SAMPLE	FORMATION	SIO2	AL2O3	FE2O3	MGO	CAO	NA2O	K2O	TIO2	MNO	P2O5	Rb	Sr	Zr
R83-2	GETH	45.82	35.65	.1	.07	.28	.08	.08	.45	<.003	.13	10	15	270
R83-3	GETH	43.24	36.48	.15	<.06	.91	.09	.24	.84	<.003	.38	10	27	138
R83-5	GETH	39.71	26.71	16.07	.26	.35	.16	.27	.59	.085	.08	<10	32	185
R83-6	GETH	36.75	26.19	4.51	2.93	7.83	.06	.38	.6	.031	.51	14	320	160
R83-7	GETH	38.44	25.26	16.55	.16	.08	.1	.27	.68	.038	.27	15	27	185
R83-8	GETH	48.53	34.1	.74	.16	.32	.38	.77	1.27	.004	.04	15	30	312
R83-9	GETH	49.8	33.31	.78	.1	.37	.06	.54	.85	.006	.33	13	33	152
R83-10	GETH	51.07	33.41	.12	.07	.13	.06	1.08	1.07	<.003	.04	13	22	312
R83-11	GETH	45.77	29.93	8.36	.18	.27	.08	.35	.82	.058	.34	15	32	200
R83-13	GETH	49.3	33.72	.26	.1	.45	.04	.37	.68	<.003	.31	10	95	200
R83-14	GETH	45.01	31.34	7.54	.2	.28	.04	.34	.85	.4	.1	13	21	223
R83-15	GETH	48.23	35.25	.36	.07	.64	.06	.38	.83	.004	.37	10	30	138
R83-20	GETH	46.14	32.48	3.58	.2	.79	.06	.28	1.01	.028	.42	11	100	152
R83-24	GETH	37.05	24.8	4.75	3.6	6.25	.2	.28	.83	.041	.27	15	63	132
R83-25	GETH	51.7	27.91	1.44	.79	1.08	.33	2.64	.62	.007	.01	32	100	127
R83-26	GETH	50.18	24.78	2.58	.81	1.37	.64	1.24	.68	.009	.02	31	132	177
R83-27	GETH	47.41	30.36	8.52	.24	.26	.08	.35	.83	.061	.03	14	45	135
R83-33	GETH	45.23	35.29	.24	.07	.33	.024	.265	1.05	.003	.16	12	30	200
R83-35	GETH	47.28	32.62	2.77	.7	.76	.008	.083	.9	.015	.45	11	70	233
R83-38	GETH	44.15	30.46	8.45	.16	.26	.016	.341	.81	.050	.19	5	20	208
R83-39	GETH	45.2	31.56	6.9	.1	.46	.022	.229	.79	.047	.4	21	40	224
R83-43	GETH	49.0	32.7	.95	.12	.31	.185	1.165	1.13	.005	.29	22	130	235
R83-44	GETH	47.18	33.39	.64	.15	.35	.128	.682	1.02	.003	.21	19	110	223
R83-45	GETH	50.36	32.95	1.06	.05	.11	.044	.105	.77	.004	.05	2	70	216
R83-46	GETH	46.4	32.93	3.77	.25	.78	.034	.197	1.1	.029	.49	12	120	271
R83-52	GETH	47.39	33.21	.61	.12	.08	.054	.635	.87	<.002	.02	33	120	275
R83-58	GETH	53.98	26.63	2.65	.19	.88	1.432	.803	.696	.025	.2	32	20	194
R83-60	GETH	50.26	31.46	2.47	.12	.21	.202	2.26	1.01	.021	.04	32	40	230
R83-64	GETH	50.87	29.78	1.95	.14	.21	.182	2.27	1.02	.012	.07	39	30	244
R83-65	GETH	44.29	33.76	8.0	<.03	<.07	.209	.086	1.46	.003	.02	5	<10	237
R83-69	GETH	47.51	32.85	1.21	.19	.08	.277	.840	.92	.006	.02	39	<10	279
R83-71	GETH	48.26	33.54	.37	.05	.34	.037	.16	1.05	<.002	.24	<15	30	249
R83-73	MOOS	44.46	32.73	2.87	.6	.34	.292	1.89	.213	.002	.04	51	190	163
R83-74	MOOS	45.37	31.99	2.91	.75	.41	.168	2.42	.425	.095	.09	60	160	376
R83-75	MOOS	45.56	33.39	1.93	.59	.31	.124	1.72	.17	.04	.01	38	110	196
R83-76	MOOS	46.57	29.53	4.42	.87	.47	.117	2.27	.488	.121	.11	75	270	282
R83-80	GETH	46.0	32.51	.96	.07	.11	.186	.175	.552	.006	.02	<15	20	223
R83-83	GETH	48.18	27.22	1.53	.97	1.78	.543	.558	.87	.013	.07	13	120	184
R83-84	GETH	48.69	30.82	1.33	.17	.15	.035	.184	.677	.009	.04	<15	20	195
R83-89	GETH	51.8	32.74	.2	.05	.56	.02	.214	.435	<.002	.45	18	70	230
R83-90	GETH	54.36	19.02	3.12	1.59	4.72	.311	2.56	.495	.02	.22	72	210	119
R83-94	GETH	48.39	32.13	.62	.23	.27	.128	.587	1.12	.005	.07	23	30	272
R83-97	GETH	48.77	33.61	.47	.06	.59	.015	.136	1.1	.002	.5	<15	125	224
R83-98	GETH	49.22	33.22	.54	.09	.1	.031	.195	1.0	<.002	.09	2	80	252
R83-105	GETH	32.62	23.62	16.92	2.79	.9	.123	.170	.89	.141	.08	13	30	247
R83-108	GETH	46.6	33.19	.94	.47	.88	.112	.389	1.1	.007	.11	6	40	265
R83-109	GETH	48.56	33.71	.62	.14	.81	.028	.258	1.15	.004	.49	4	150	268
R83-114	GETH	44.44	35.9	.26	.07	<.04	.06	.18	1.09	<.004	.03	<15	20	243
R83-115	GETH	46.11	36.1	.17	.06	.15	.19	.08	.94	<.004	.08	4	20	207
R83-121	MOOS	18.03	9.4	6.83	10.26	21.36	.21	.45	.28	.056	.27	25	250	67
R83-122	MOOS	29.74	23.32	4.87	5.19	11.83	.12	.26	.56	.020	.57	24	450	164
R83-134	GETH	36.42	25.24	5.24	3.75	6.55	.17	.25	.97	.047	.24	13	120	162
R83-151	MOOS	48.65	30.12	2.72	1.17	1.58	.73	2.83	.4	.079	.08	71	340	360
R83-156	MOOS	47.92	34.71	1.47	.6	.25	.63	1.72	.18	.02	.06	59	370	186
R83-159	BLUE	35.0	22.2	18.42	.62	.1	.54	2.02	.27	<.003	<.02	29	150	561
R83-174	GETH	49.04	31.72	1.06	.14	.13	.07	1.02	.84	.008	.05	8	25	218
R83-194	MOOS	47.42	29.33	4.67	1.23	.42	.94	2.89	.2	.013	.02	79	120	329
R83-205	GETH	48.02	34.74	.36	.08	.37	<.03	.12	.98	<.004	.26	<15	65	238
R83-207	MOOS	45.99	30.87	2.04	.83	2.45	1.11	3.32	.47	.015	.06	81	180	545
R83-208	MOOS	46.84	34.5	1.0	.53	.21	.98	1.97	.17	<.003	.03	41	140	195

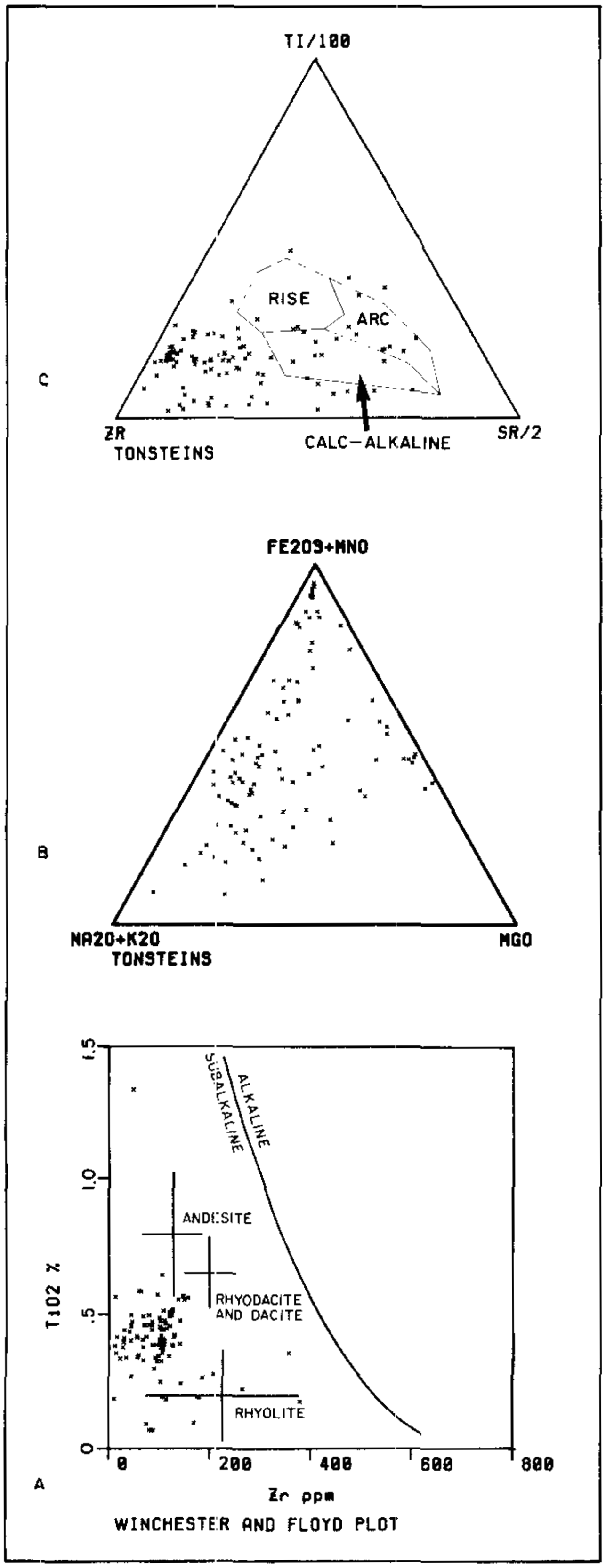

Figure 20-2. Diagnostic plots of chemical values. (a) AFM diagram. (b) Zr:Ti:Sr diagram. (c) TiO_2:Zr diagram.

elements from the total population of 101 samples analysed to date. There are no significant differences between this matrix and the one reported in Kilby (1985). A significant value in this matrix would have a correlation value greater than 0.26 or less than −0.26 at the 99 per cent confidence level. A series of plots were prepared from the chemical data in an attempt to predict the general original composition of these rocks and to determine the presence of any natural groupings (Fig. 20-2). The Ti:Zr plot suggests an original composition in the rhyolite to andesite range. The ternary plot of Ti:Zr:Sr shows the majority of the strata falling outside common zones. This may suggest a general depletion of Sr. If strontium were added to the samples, the majority would fall in the calc-alkaline zone. Strontium tends to substitute for calcium due to similar ionic size and charge. It will be shown following that ankerite contains a significant portion of the total strontium. It is felt that strontium was mobile and tended to be lost from the original minerals although some was retained in the post-deposition mineral ankerite.

The AFM diagram shows widely scattered data. This scatter is due in part to the late introduction of MgO in the form of ankerite (discussion following).

Early attempts at correlation based on chemical values proved encouraging on a local scale (Kilby, 1985). For regional correlations it is important to consider only the elements or ratios of elements that are not affected by diagenesis. It was suggested (Kilby, 1985) that calcium and magnesium in the form of ankerite had been introduced in a significant number of the samples. It is felt that although these elements and strontium were useful in local correlations where similar burial histories could account for their introduction, their effects should be removed before any regional correlations are attempted.

The resources required to chemically analyse all samples collected in this study could not be justified. Consequently an X-ray diffraction procedure was devised as an alternative, more cost-effective comparison method.

X-RAY MINERALOGY

X-ray diffraction analysis was performed on all samples collected during this study. Mineral identification and relative abundances were determined by J. Kwong in the Ministry Laboratory. To quantify the X-ray diffractogram chart information for comparative purposes a system was developed to digitally record the curve shapes and store this information for subsequent analysis. Digitization of X-ray diffractograms provides the facility to compare the shapes of the diffractogram curves and compare peak intensities for specific minerals, enabling prediction of chemical composition.

X-RAY DIFFRACTOGRAM DIGITIZING

Kilby (1985) pointed out the visual similarities of X-ray diffractogram curves for samples which had been correlated by both chemical and geophysical means. The first step in utilizing these diffractograms quantitatively was to digitize the curves by means of a digitizing tablet connected to an IBM XT microcomputer. Program CURV-DIG (Kilby, 1984b) was used to collect the digital data. The diffractogram was digitized between the interval 5 to 40 degrees 2θ (Cu kα; Fig. 20-3a). The chart tracing was followed with the digitizer stylus and data points were recorded at 0.127-centimetre spacings along the trace. Typically 1100 to 1200 coordinate pairs were collected for each curve. This raw data was then reduced and standardized with the program CURV-RED (Kilby, 1984b). CURV-RED aligned each curve about the quartz peak at 26.6 degrees 2θ and calculated the height in millimetres of the curve at 0.1 degree 2θ intervals for the 345 points between 5.1 and 39.5 degrees 2θ (Fig. 20-3b). These reduced data were stored in Data Handler format to be accessed by the analysis programs of the Cal Data Geological Analysis package. The reduced data were then used to plot a curve at the same scale as the original for verification. Any deviations

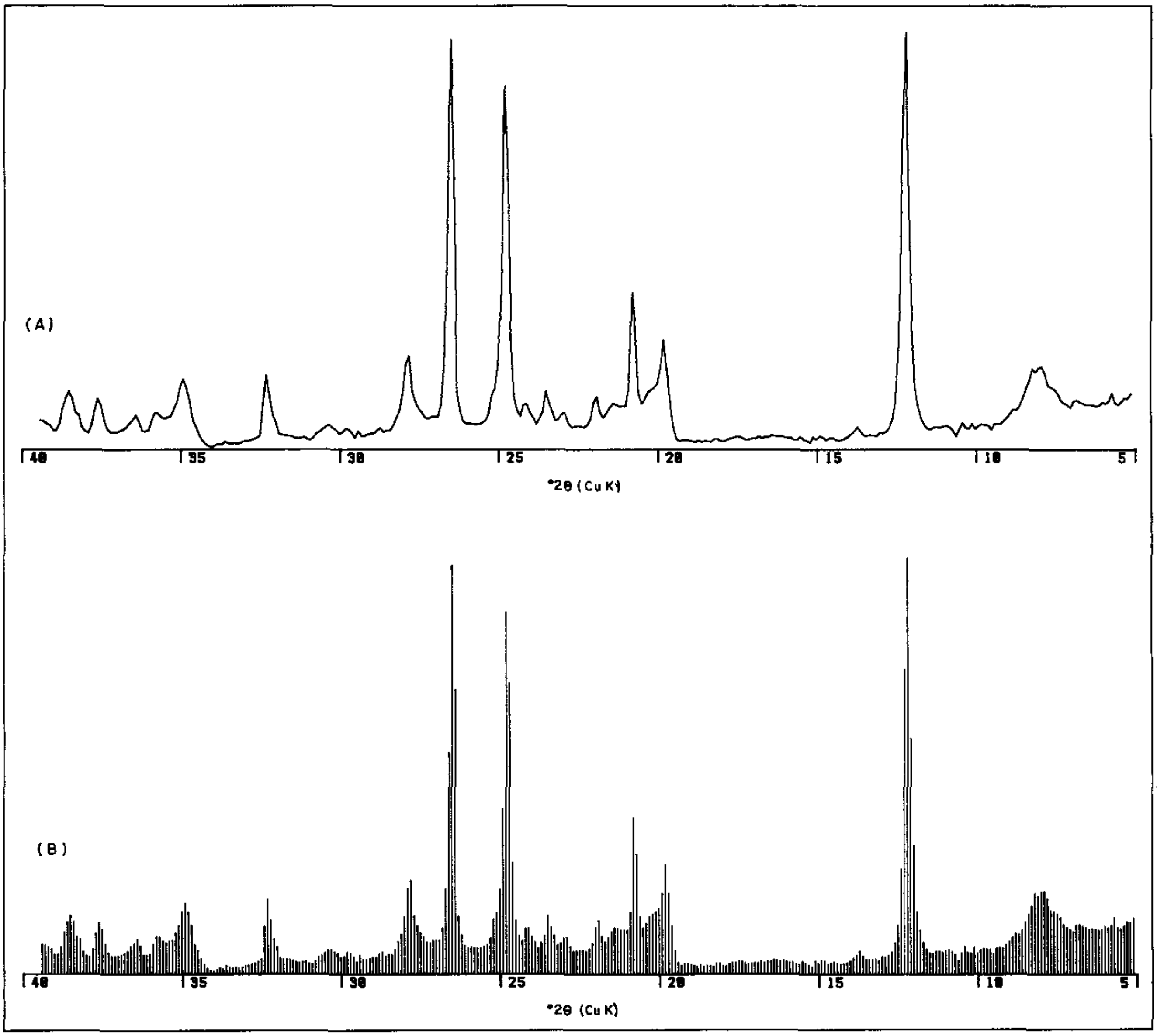

Figure 20-3. (a) Example of an X-ray diffractogram. (b) Positions and heights of points saved for each curve. Heights range from 0 to 2 500 millimetres.

between the two curves were easily identified by overlaying them. Corrections were made to the pertinent data point with the editor of the Data Handler.

The X-ray diffractogram was divided into 17 zones of 0.4 degree 2θ width which corresponded to prominent peaks on the curve which represent common tonstein and bentonite minerals (Table 20-2); each zone, therefore, is treated as a 'pseudomineral.' The total of the four curve point heights above background within these zones were used to quantify the abundance of the pseudominerals. Background was defined by two straight lines; one running from the curve height at 10 degrees 2θ to 15 degrees 2θ, the other from 15 degrees 2θ to 34 degrees 2θ. The absolute values of the areas under the portion of the curve assigned to each pseudomineral do not directly correspond to the abundances of real minerals because of varying absorption coefficients and other factors. The pseudomineral zones do, however, provide a means of examining relative changes in mineral abundances.

A variety of correlation procedures are possible with the pseudomineral data but present work is concentrating on determining which pseudominerals or which portions of the X-ray diffractogram are most diagnostic for a variety of purposes such as: *regional correlation, identifying secondary carbonatization, identi*fying secondary silicification, distinguishing weathered samples, and tonstein and bentonite differentiation.

PSEUDOMINERAL EXAMINATION

An initial examination employing the pseudomineral method was carried out on the 101 chemically analysed samples. Figure 20-4 displays the correlation matrix for the 17 pseudominerals. Any correlation coefficient greater than 0.26 or less than −0.26 is significant at the 99 per cent confidence level. High correlation coefficients between adjacent pseudomineral zones are suspect and likely due to overlapping of peaks or wide peaks sampled by two pseudomineral zones. The usefulness of correlation coefficients is

TABLE 20-2
PSEUDOMINERALS FOR TONSTEINS AND BENTONITES, PEACE RIVER COALFIELD

Pseudomineral	Degree 2θ (Cu kα)
Goethite	33.1 – 33.4
Pyrite	32.8 – 33.1
Siderite	31.9 – 32.2
Ankerite	30.7 – 31.0
Calcite	29.3 – 29.6
Barite	28.6 – 28.9
Feldspar	27.7 – 28.0
Quartz	26.4 – 26.7
Septechlorite	18.5 – 18.8
Gorceixite	15.3 – 15.6
Harmotome	13.6 – 13.9
Kaolinite	12.1 – 12.4
Gypsum	11.4 – 11.7
Illite	8.6 – 8.9
Montmorillonitic mixed-layer clay	7.9 – 8.2
Illitic mixed-layer clay	7.4 – 7.7
Chlorite	5.6 – 5.9

not affected by the fact that the pseudomineral values do not represent true mineral abundances — so long as the zones reasonably represent specific minerals, the correlation coefficients will be similar to the values obtained for true mineral quantitites.

Several pseudomineral abundance relationships are apparent from the correlation matrix tabulation. The diffractogram results for the pseudomineral goethite correlates strongly with those for pyrite and ankerite. This suggests an alteration of pyrite to goethite, however, the diagnostic X-ray peaks for these minerals are close together, and may overlap to some extent, causing spuriously high correlation values. The ankerite-goethite peaks are well separated so the high correlation is real and due to the introduction of secondary carbonate (discussed later). Siderite does not significantly correlate with any other pseudomineral. Ankerite has a strong positive correlation with goethite, discussed previously, and a signficant negative correlation with kaolinite. Calcite and barite are strongly correlated but this may be due to the closeness of the peaks. Calcite has strong positive correlations with illite and the mixed-clay minerals but a strong negative correlation with kaolinite. This suggests that the presence of calcite is related to the same processes which lead to formation of smectite-rich bentonites rather than kaolinite-rich tonsteins. The marine affinity of bentonites is consistent with the presence of calcite in this type of alteration. Feldspar has strong positive correlations with the mixed-layer clays and a negative correlation with kaolinite. Kaolinization strongly affects feldspar while the processes that create smectite clays appear to affect it less. Feldspar and harmotome have a strong correlation but this is likely due to the fact that some feldspars have secondary peaks which coincide with the harmotome zone. Quartz has significant positive correlations with feldspar and illite. Quartz and feldspar peaks are well separated so their correlation is significant. The correlation with illite suggests that silica is released during diagenesis as smectite is converted to illite. Septechlorite and gorceixite are not positively or negatively correlated with any of the other pseudominerals. Kaolinite has a strong correlation with gypsum but this is almost certainly due to the proximity of the two diffraction peaks. Kaolinite displays strong negative correlations with the minerals that characterize bentonites—illite, montmorillonitic mixed-layer clay, illitic mixed-layer clay, and chlorite. Kaolinite also has strong negative correlations with calcite, ankerite, and goethite. Gypsum has negative correlations with virtually all of the pseudominerals except kaolinite, as discussed previously. Field examination of some gypsum-rich samples revealed gypsum rosettes on fracture surfaces.

Illite has three previously discussed positive correlations — with calcite, barite, and quartz. In addition it has strong positive correlations with the mixed-layer clays. Illite commonly forms from the collapse of interlayer spaces in mixed-layer clays; thus the more smectite the more potential for illite formation. Montmorillonitic mixed-layer clay has a very high correlation with illitic mixed-layer clay which is in part due to the broadness and nearness of their respective peaks. Chlorite has strong negative correlations with kaolinite and gypsum.

Several significant trends in mineralogy are indicated by the correlation matrix. Ankerite and goethite exist in samples at the expense of all other minerals, which suggests they formed later. Siderite is unrelated to all other minerals and is likely a weathering product. Calcite and barite are strongly correlated and preferentially concentrated in the environment which produces illite and smectite. Feldspar, which is believed to be primary, survives in the bentonite-producing environment but is altered to kaolinite in the tonstein-producing environment. Quartz content is closely correlated with feldspar; it also is likely predominantly primary; however, a strong

GEOTHITE	PYRITE	SIDERITE	ANKERITE	CALCITE	BARITE	FELDSPAR	QUARTZ	SEPTOCHLORITE	GORCEIXITE	HARMOTOME	KAOLINITE	GYPSUM	ILLITE	MONT. M/C	ILLITIC M/C	CHLORITE	
0	.673	-.091	.5	.148	.047	-.252	-.132	-.115	-.05	-.151	-.354	-.279	.196	0	-.064	-.055	Geothite
0	0	-.023	.012	.05	.17	-.077	-.105	-.069	-.094	-.099	-.195	-.101	0	.051	.05	-.055	
0	0	0	-.042	-.022	0	-.01	-.117	-.079	.068	-.074	.054	-.039	-.054	.102	0	-.134	
0	0	0	0	.122	-.313	-.129	-.168	-.161	-.014	-.093	-.357	-.329	-.039	-.068	-.116	-.056	
0	0	0	0	0	.474	.147	.089	0	-.065	-.081	-.48	-.27	.345	.471	.304	.089	•
0	0	0	0	0	0	.275	.232	.252	-.026	-.044	-.243	.062	.518	.6	.481	.078	
0	0	0	0	0	0	0	.272	.059	0	.556	-.212	-.114	.112	.5	.472	.106	
0	0	0	0	0	0	0	0	-.014	-.033	.142	-.012	-.015	.275	.078	-.003	-.079	
0	0	0	0	0	0	0	0	0	.101	.073	.003	.224	.046	.064	.055	0	•
0	0	0	0	0	0	0	0	0	0	.244	.121	.147	-.151	-.143	-.193	-.204	
0	0	0	0	0	0	0	0	0	0	0	.094	.038	-.07.	.065	.135	.106	
0	0	0	0	0	0	0	0	0	0	0	0	.704	-.302	-.527	-.543	-.41	
0	0	0	0	0	0	0	0	0	0	0	0	0	-.198	-.314	-.374	-.409	
0	0	0	0	0	0	0	0	0	0	0	0	0	0	.435	.309	.243	•
0	0	0	0	0	0	0	0	0	0	0	0	0	0	0	.811	.396	
0	0	0	0	0	0	0	0	0	0	0	0	0	0	0	0	.681	
0	0	0	0	0	0	0	0	0	0	0	0	0	0	0	0	0	Chlorite

Figure 20-4. Correlation matrix of 17 pseudominerals calculated for 101 samples.

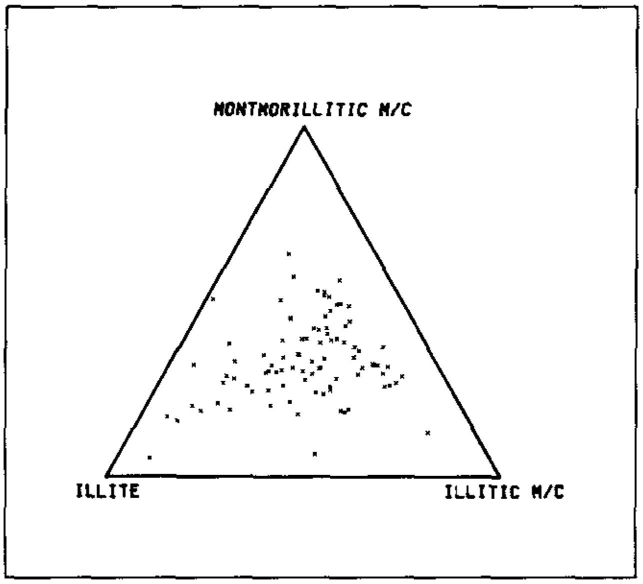

Figure 20-5. Ternary plot showing the relationship between the pseudominerals illite, montmorillonitic mixed-layer clay, and illitic mixed-layer clay.

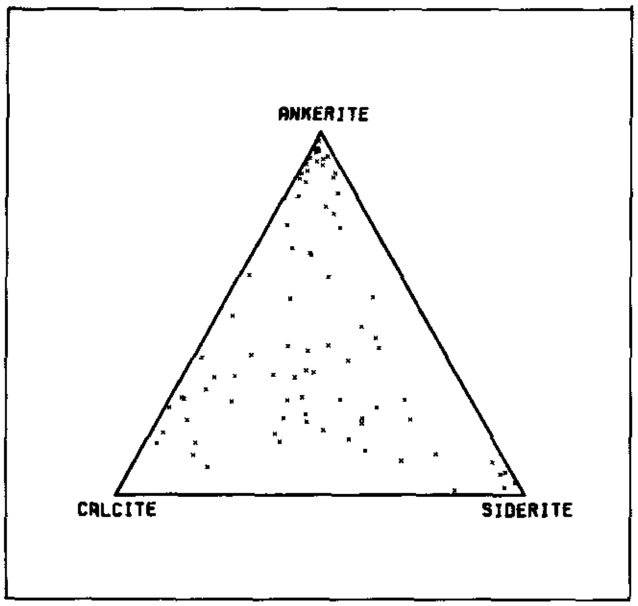

Figure 20-6. Ternary plot of the relative quantities of the major carbonate pseudominerals.

positive correlation with illite suggests some is secondary. Kaolinite, which characterizes tonsteins, apparently replaces all other minerals. Illite, chlorite, and the mixed-layer clays correlate in a similar manner to virtually all other minerals; these clay minerals characterize bentonites.

The ternary plot of illite and the two mixed-layer clays (Fig. 20-5) shows a relatively constant ratio (1:1 ±) between the mixed-layer clays as the illite content varies. The ternary plot of the carbonate minerals calcite, ankerite, and siderite for the 101 samples shows a relatively even distribution of the three minerals, although some samples have high concentrations of ankerite and siderite (Fig. 20-6). In this data, points which plot in the centre of the diagram generally represent samples with little or very low amounts of these carbonates.

CORRELATION OF CHEMICAL AND X-RAY ANALYTICAL RESULTS

The digitized X-ray diffractorgram data allowed a correlation study between the diffractogram curves and the chemical analyses of the 101 samples. Each of the 345 curve-defining points were correlated with each of the 13 elements analysed for each sample. The result was 345 correlation coefficients which covered the full length of the digitized diffractograms for each element based on 101 samples. The correlation coefficients then were plotted against the 2θ angles. The resultant plots (Fig. 20-7) show the correlation between elements and minerals within the 101 samples. By examining the 2θ angles which correspond to a specific mineral, elemental relationships for that mineral can be determined. Also the plots

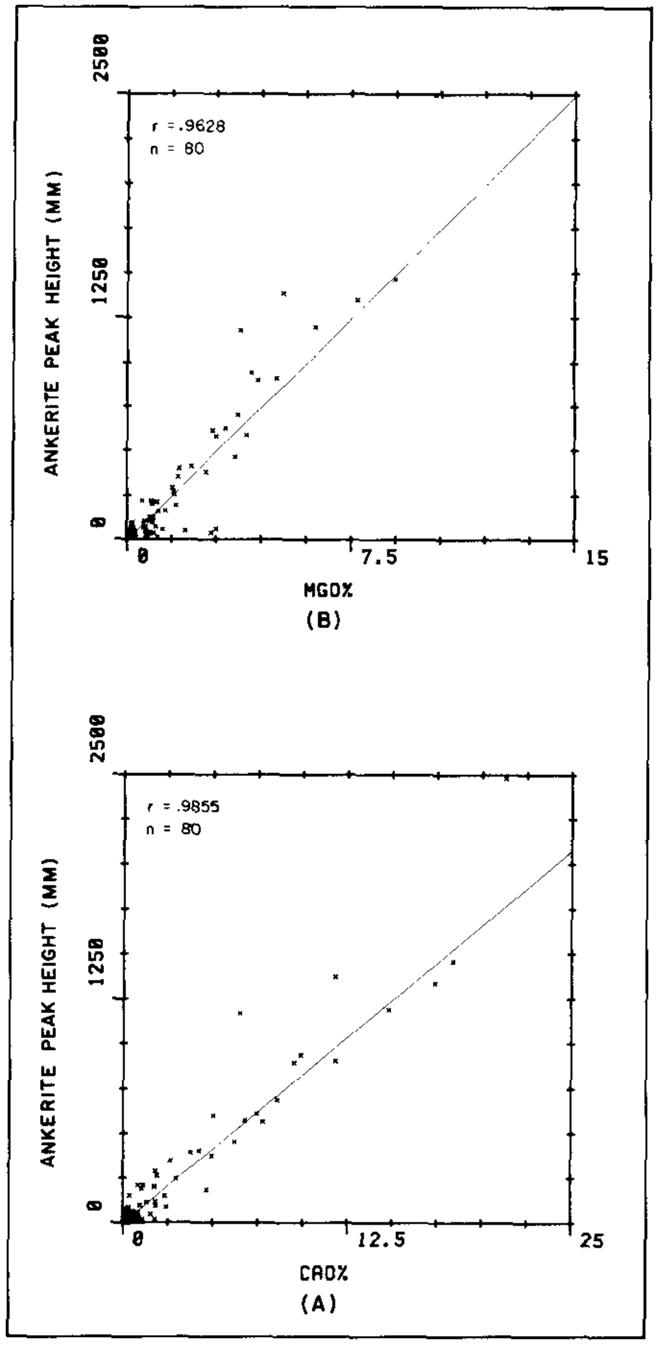

Figure 20-8. Cross-plots showing the relationship between the mineral ankerite (30.8 degrees 2θ on X-ray diffractograms) and (a) CaO per cent and (b) MgO per cent.

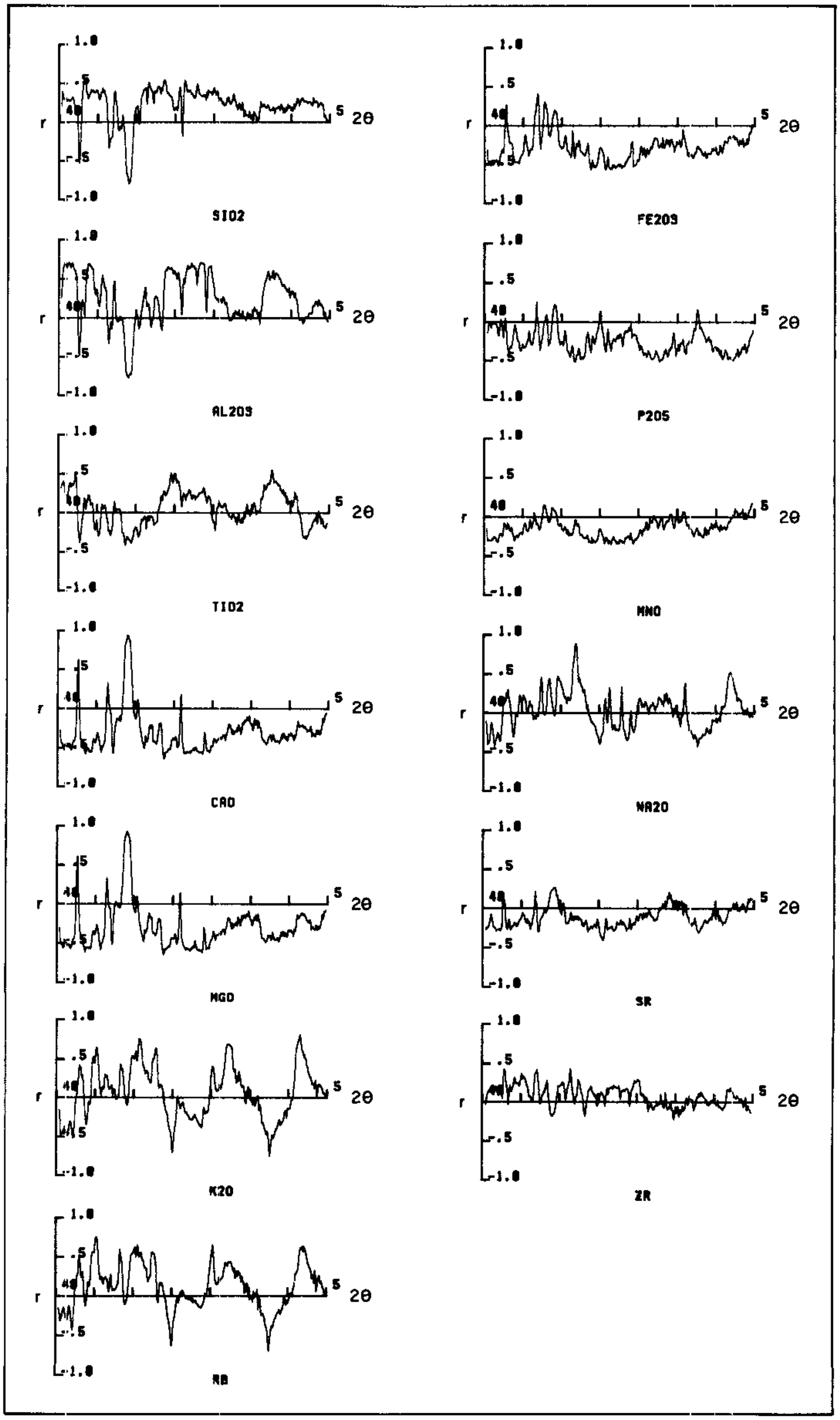

Figure 20-7. Correlation coefficent plots of X-ray diffractogram relationships with chemical abundances for 13 elements based on 101 samples.

illustrate which minerals contain the various elements. Significant correlations correspond to coefficients greater than 0.26 or less than −0.26.

Comparison of CaO and MgO correlation curves show the two elements to have virtually identical correlation coefficients throughout the range of minerals covered by the diffractogram. The prominent peak at 30.8 degrees 2θ corresponds to ankerite. The extremely high correlation coefficients of 0.986 and 0.963 (Fig. 20-7) for calcium and magnesium imply that virtually all of these two elements occur in the same mineral — ankerite — which is an alteration mineral.

Figure 20-8 shows the relationships between calcium and magnesium with respect to the height of the ankerite peak at 30.8 degrees 2θ. From these plots it is also a simple matter to calculate the magnesium to calcium ratios found in ankerite. Based on the linear regression equations the ratio of MgO to CaO in ankerite is 0.475. The ankerite:magnesium plot shows some samples with MgO around 2 to 3 per cent with no ankerite peak, which suggests the presence of some other magnesium-bearing mineral.

Potassium and rubidium have similar correlation curves (Fig. 20-7). Strong correlations in the 26.7 to 30.5-degree 2θ range imply significant correlation of potassium and rubidium with the feldspars. A sharp decrease at 28 degrees 2θ (sodic feldspars) corresponds to a strong positive correlation in the sodium curve. Both potassium and sodium also correlate well with the smectite peak around 8 degrees 2θ, suggesting alteration of feldspars to these clays. The relationship between potassium and rubidium does not change between feldspar and smectite. Rubidium commonly substitutes for potassium; it has the same charge and a similar ionic radius. The substitution of rubidium for potassium may be one of the reasons for the high gamma log responses often seen for bentonites. Taking into account the respective half lives and the percentage of radioactive isotopes of each element, rubidium is about 3.46 times as radioactive as potassium. Potassium, rubidium, and sodium show strong negative correlations with kaolinite (25 and 12.3 degrees 2θ). This negative correlation explains why, in contrast to the strong gamma log responses noted for smectite-rich bentonite, kaolinite-rich tonsteins have very weak responses. The close association of potassium and rubidium may proved useful in correlating bentonites with similar Rb/K ratios; Figure 20-9 contains a cross-plot showing the relationship of these two elements.

Alumina and silica have similar correlation curves which are nearly mirror images of the calcium and magnesium curves, suggesting these two sets of elements tend to be mutually exclusive in these samples. Titanium has a curve which shows correlations similar to those of alumina and silica with respect to the various minerals. Titanium and alumina have similar correlations with respect to kaolinite at 12.5 and 25 degrees 2θ.

Managanese and strontium have very few significant correlations but their general traces are similar. Both are negatively correlated with kaolinite. Strontium has a low positive correlation with ankerite at 31 degrees 2θ. This results from strontium substituting for calcium as discussed previously.

Iron and phosphorous have similarly shaped curves in the 30 to 35-degree 2θ range; there are many overlapping mineral peaks in this interval, such as ankerite and apatite. Phosphorous shows slight positive correlation with kaolinite.

CHEMICAL ESTIMATES FROM X-RAY CURVES

The correlation curves (Fig. 20-7) show which minerals contain various elements. Both positive and negative correlations provide useful information about elemental abundances in given minerals. If an element is found exclusively in a single mineral then a simple cross-plot (Fig. 20-8) will show the relationship and provide a predictive tool for element contents. However if an element occurs in several minerals or is negatively affected by the presence of some other mineral, then a slightly more complicated technique such as multiple linear regression must be employed.

Multiple linear regression proved successful in determining which peaks most accurately described the abundances of various elements and at arriving at a predictor equation. All multiple linear correlations were based on only 80 samples, due to limited memory capacity of the available microcomputers. Plots of the results of the derived equations contain all 101 samples.

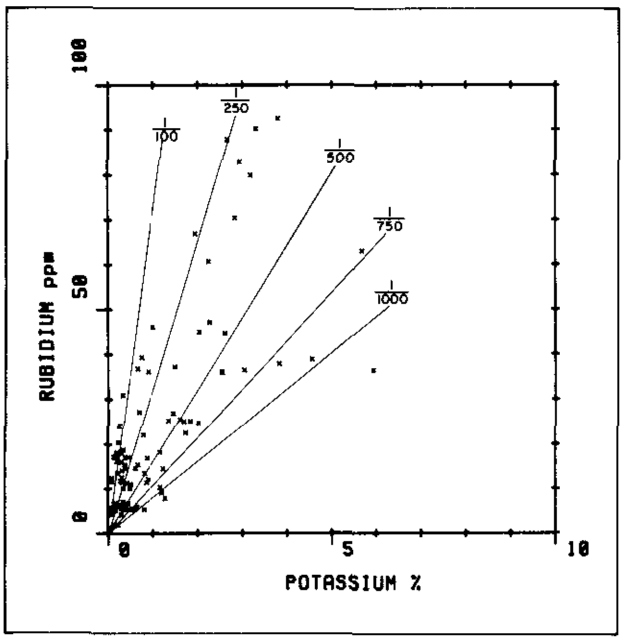

Figure 20-9. Cross-plot showing the relationship between Rb and K_2O content. Rubidium/potassium ratios are also displayed.

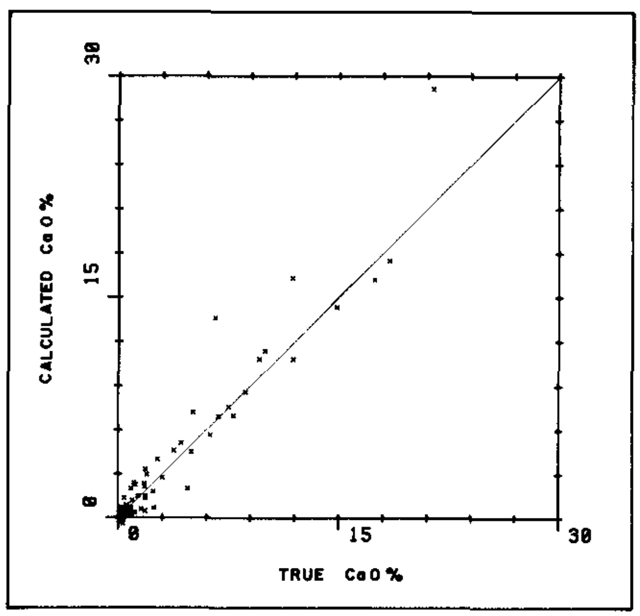

Figure 20-10. Comparison of X-ray calculated CaO content from multiple linear regression and chemical analysis. Regression based on 80 samples, 101 plotted.

Calcium was shown previously (Fig. 20-8a) to have a very strong correlation with the X-ray curve at 30.8 degrees 2θ. Examination of the correlation curve for calcium (Fig. 20-7) shows that a strong negative correlation occurs at 26.1 degrees 2θ, which is an area influenced by both quartz and kaolinite. Utilization of both the curve positions, 30.8 and 26.1 degrees, provided only marginally better definition of the calcium content than the 30.8-degree peak alone ($R = 0.9855$ to $R = 0.9876$). Figure 20-10 contains a comparison of the chemical analysis values with those predicted from ankerite and the quartz-kaolinite peaks. The extremely small increase in resolution does not justify inclusion of the second peak in the predictor equation. CaO per cent values are adequately described by the linear regression equation:

$$\text{CaO\%} = -0.159928 + 0.012078 \text{ (peak height at } 30.8^\circ\ 2\theta)$$

This equation explains 97 per cent of the calcium variance in the samples. The similarity of the correlation curves suggest that a similar equation would provide an equally good estimate of magnesium content. Based solely on the ankerite peak at 30.8 degrees 2θ, 92.7 per cent of the magnesium variance is explained by the following equation:

$$\text{MgO\%} = 0.0898353 + 0.00534672 \text{ (peak height at } 30.8^\circ\ 2\theta)$$

In this case the multiple linear regression technique showed that a single mineral was the best estimator of two elements, CaO and MgO.

Potassium content was found to be predicted best by a combination of three curve positions. The curve positions at 29.1, 12.3, and 8.4 degrees correspond to the minerals potassium feldspar, kaolinite, and illite, respectively. The respective correlation coefficients of each of these positions with K_2O content was +0.7957, −0.6738, and +0.8569. Figure 20-11 contains the true and calculated results of predicator equations based on several combinations of these minerals. It is interesting that the two positively correlated minerals (Fig. 20-11a) do not predict K_2O content as well as a combination of a positively and negatively correlated mineral (Fig. 20-11b); the best predictor utilized all three minerals. This equation, which explained 89 per cent of the K_2O variance was:

$$K_2O\% = 0.0775335 + 0.00809 \text{ (peak height at } 29.1^\circ) + 0.009951 \text{ (peak at } 8.4^\circ) + -0.000594 \text{ (peak height at } 12.3^\circ)$$

The fact that both feldspar and illite give good estimates of K_2O content but when combined do not greatly improve the estimate of K_2O content suggests these minerals are directly related. This relationship is the result of concordant increases in feldspar and illite peaks; illite is an alteration product of feldspar. Rubidium content would be accurately predicted by a similar equation due to the similarity between the Rb and K_2O correlation curves.

The sodium correlation curve (Fig. 20-7) showed a strong positive correlation with sodium feldspar at 28 degrees 2θ. A significant negative correlation occurs with kaolinite at 12.4 degrees 2θ, and a moderate positive correlation is present with illite at 7.9 degrees 2θ. Individual correlations with these three peaks were 0.9202, 0.2201, and 0.5774 for feldspar, kaolinite, and illite, respectively. The combination of feldspar and kaolinite at $R = 0.9314$ proved a better estimate than feldspar and illite at $R = 0.9205$ (Fig. 20-12). Inclusion of the illite peak did not significantly improve the predictability of NaO content so only two peaks were used in the following equation, which explains 86.7 per cent of the variance of sodium:

$$\text{NaO\%} = -0.00420716 + 0.00559678 \text{ (peak height at } 28.2^\circ) + -0.0000779881 \text{ (peak height at } 12.4^\circ)$$

The correlation curve for Al_2O_3 content (Fig. 20-7) has a large range of positively correlation points on the X-ray curve and one strong negative correlation. The negative correlation coincides with ankerite and has a value of −0.7727. Points which corresponded to feldspar and kaolinite, 21.3 and 12.2 degrees, were selected arbitrarily from the myriad of positive correlations. Correlation co-

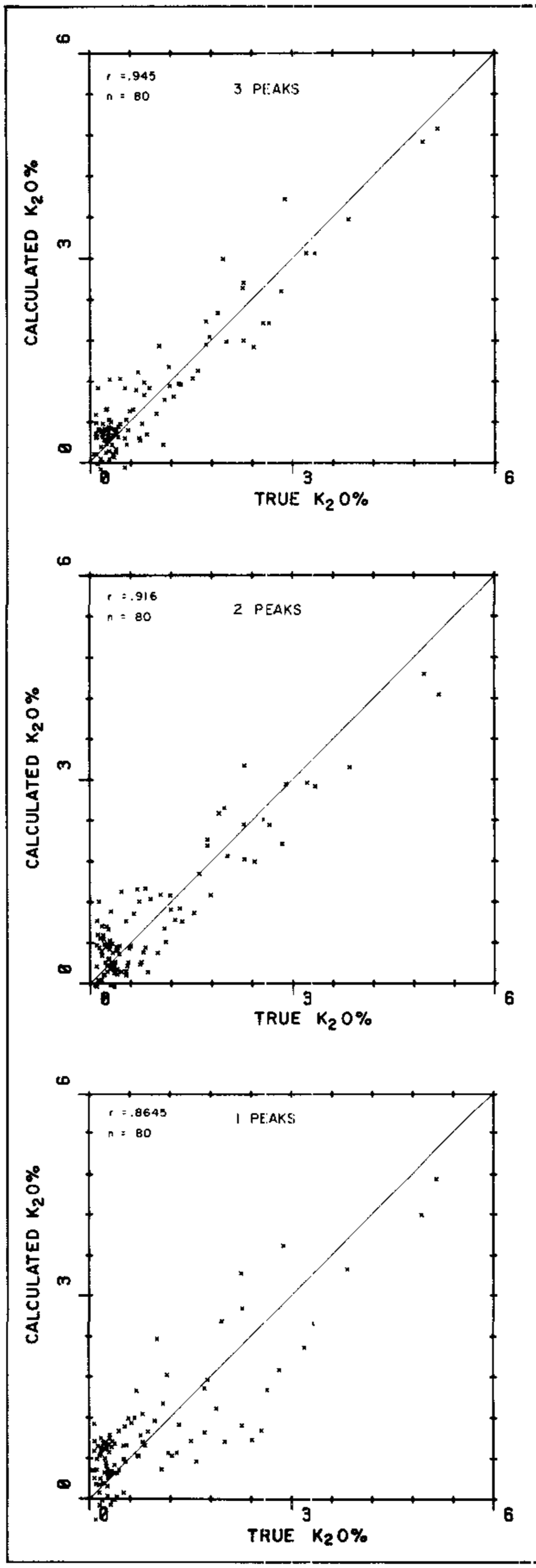

Figure 20-11. Examples of predictive regression equations for K_2O content based on up to three points on the diffractograms.

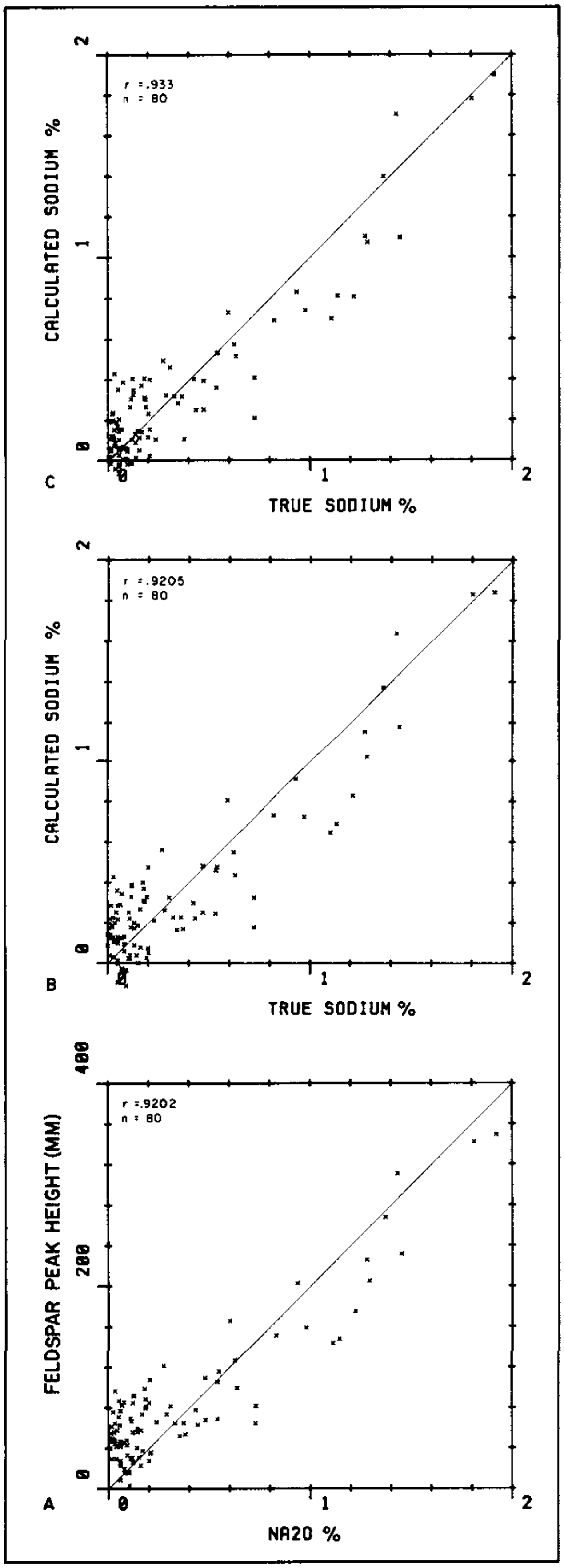

Figure 20-12. Na_2O% predictability (a) based on one curve point, (b) based on two curve points, and (c) based on three curve points.

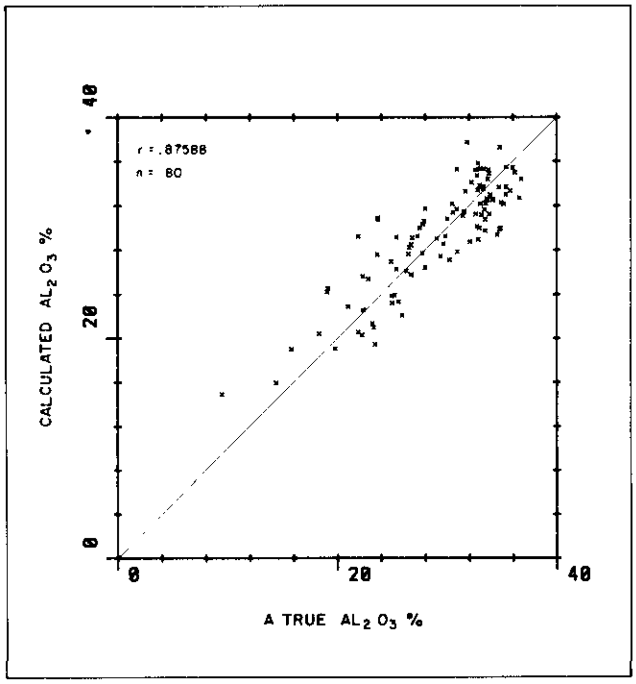

Figure 20-13. Predictability of Al_2O_3 content based on three X-ray curve positions.

efficients of 0.7176 and 0.6885 were obtained for feldspar and kaolinite. A predictor equation based on all three peaks explained 77 per cent of the variance of Al_2O_3. Figure 20-13 contains the true values and those calculated using the following equation:

$Al_2O_3\% = 23.6822 + -0.008284$ (peak height at 30.9°) + 0.017914 (peak height at 21.3°) + 0.002358 (peak height at 12.2°)

In this case ankerite, a mineral containing no aluminum, proved to be the best single predictor. This is due to the dilution effect of late ankerite mineralization, which simply reduces the percentage of aluminum-bearing minerals. Ankerite and kaolinite mineral peaks explained 73 per cent of the Al_2O_3 variance; the addition of feldspar brought this value up to 77 per cent.

CONCLUSIONS

This article has shown the viability of using X-ray diffractograms to accurately predict sample chemistry. In some aspects the diffractograms are superior correlation tools because they not only provide mineralogical information but also many of the same correlation properties as chemical data. The objective of this part of the study was to find an alternative to chemical analysis; X-ray diffraction provides one.

Techniques developed for this study provide insight into the various styles of alteration affecting volcanic ash falls in and around coal swamps. The chemical-diffractogram correlation curves also provide a means of examining the chemical characteristics of individual minerals within a sample. Certain elements, such as calcium and magnesium, can be shown to have been introduced largely with one mineral, ankerite, at a late date. These elements are obviously of no use for regional correlation of an ash band on the basis of common source chemistry.

Future work will concentrate on applying the knowledge of chemical behaviour of these rocks to their regional correlations. Comparisons of altered samples with similar mineralogy (that is, ankerite rich) may give insight into the causes or mechanisms of the alteration. Comparisons of coal rank and mixed-layer clay abundances may aid the understanding of clay diagenesis.

ACKNOWLEDGMENT

All X-ray diffraction analyses were performed by Dr. J. Kwong of the Ministry Laboratory and his efforts are greatly appreciated.

REFERENCES

Duff, P.McL.D. and Gilchrist, R. D. (1983): Correlation of Lower Cretaceous Coal Measures, Peace River Coalfield, British Columbia, *B.C. Ministry of Energy, Mines & Pet. Res.*, Paper 1981-3, 31 pp.

Kilby, W. E. (1984a): Tonsteins and Bentonites in Northeast British Columbia (93O, P, I), *B.C. Ministry of Energy, Mines & Pet. Res.*, Geological Fieldwork, 1983, Paper 1984-1, pp. 95-107.

——— (1984b): CURV-DIG and CURV-RED, BASIC Programs, unpub., *B.C. Ministry of Energy, Mines & Pet. Res.*

——— (1985): Tonstein and Bentonite Correlation in Northeast British Columbia (93P, I; 94A), *B.C. Ministry of Energy, Mines & Pet. Res.*, Geological Fieldwork, 1984, Paper 1985-1 pp. 257-277.